

**EFFECT OF LONG-PERIOD OCEAN TIDES  
ON THE EARTH'S POLAR MOTION**

by

Richard S. Gross\*, Ben F. Chao<sup>†</sup>, and Shailen D. Desai\*

\*Jet Propulsion Laboratory  
California Institute of Technology  
Pasadena, California 91109-8099

<sup>†</sup>Goddard Space Flight Center  
Greenbelt, Maryland 20771

Corresponding Author:

Richard S. Gross  
Jet Propulsion Laboratory  
Mail Stop 238-332  
4800 Oak Grove Drive  
Pasadena, CA 91109-8099, USA  
ph: +1 818-3544010  
fax: +1 818--393-6890  
rsg@logos.jpl.nasa.gov

Thursday, January 23, 1997

10 be submitted to *Progress in Oceanography*

# Effect of Long-Period Ocean Tides on the Earth's Polar Motion

Richard S. Gross\*, Ben F. Chao<sup>†</sup> and Shailen D. Desai\*

\*Jet Propulsion Laboratory, California Institute of Technology, Pasadena, CA

<sup>†</sup>Goddard Space Flight Center, Greenbelt MD

**Abstract.** The second-degree zonal tide raising potential is symmetric about the polar axis and hence can excite the Earth's polar motion only through its action upon nonaxisymmetric features of the Earth such as the oceans. In the long-period tidal band, spectral peaks occur at the fortnightly tidal frequencies in power spectra of polar motion excitation observations from which atmospheric effects have been removed. Different observed polar motion excitation series are studied, and different methods of removing atmospheric effects from the polar motion excitation observations are explored in order to assess the robustness of the resulting empirical models for the observed effect of long-period ocean tides on polar motion excitation. At fortnightly frequencies, the various observed empirical models are found to agree with each other to within about  $1\sigma$ . The observations are then compared with predictions of three ocean tide models: two purely hydrodynamic models and one in which Topex sea surface height measurements have been assimilated. At the fortnightly tidal frequencies, the three ocean tide models predict polar motion excitation amplitudes that differ from each other and from the observations by factors as large as 2, and phases that differ by more than 1000. This illustrates the need for improved models for the effect of long-period ocean tides on polar motion excitation.

## INTRODUCTION

Since the Earth's rotation axis is not aligned with its symmetry axis, the Earth wobbles as it rotates. This wobbling motion of the solid Earth, also known as polar motion, is forced by (1) exchange of nonaxial angular momentum between the solid Earth and the Earth's fluid components, and by (2) deformation of the solid Earth (for reviews see, e.g., MUNK and MACDONALD, 1960; LAMBUCK, 1980, 1988; MORITZ and MUELLER, 1988; EUBANKS, 1993).

Tidally induced deformation of the solid Earth causes changes in the Earth's rate of rotation (e.g., YODER, WILLIAMS and PARKE, 1981); but since the tide-raising potential is symmetric about the polar axis, tidally induced deformations of the axisymmetric solid Earth cannot cause polar motion. However, due to the nonaxisymmetric shape of the coastlines, the tide-raising potential acting on the oceans can generate polar motion via exchange of nonaxial ocean tidal angular momentum with the solid Earth.

The observed polar motion at nearly diurnal and semidiurnal frequencies has been shown to be dominantly caused by ocean tidal forcing (HERRING, 1993; SOVERS, JACOBS and CROSS, 1993; HERRING and DONG, 1994; WATKINS and EANES, 1994). CHAO (1994) and GROSS, HAMDAN and BOGGS (1996) have recently presented evidence that ocean tides in the long-period tidal band also measurably cause polar motion, particularly at fortnightly frequencies. This report extends the earlier results of CHAO (1994) and GROSS, HAMDAN and BOGGS (1996) by utilizing improved polar motion and atmospheric angular momentum data sets that have recently become available, by exploring different means of removing atmospheric effects from the polar motion observations prior to extracting the ocean tidal effects, and by comparing the observed ocean tidal effect on polar motion with that predicted not only by purely hydrodynamic ocean tide models, but also by a model that has assimilated Topex sea level height measurements (DESAI, 1996). The methodology employed in this report is only briefly described here since it closely follows that of GROSS, HAMDAN and BOGGS (1996) to which interested readers are referred for greater detail.

## **OBSERVATIONS**

### **Polar Motion Excitation Data**

The complex-valued polar motion excitation function, or *chi*-function, is the polar motion forcing function that, at frequencies far from the Free Core Nutation resonance (a resonance in polar motion of nearly diurnal frequency), is related to polar motion through the expression (e.g., GROSS, 1992):

$$\mathbf{p}(t) + \frac{t^c}{\sigma_{cw}} \frac{d\mathbf{p}(t)}{dt} = \chi(t) \quad (1)$$

where  $i \equiv d-l$ ,  $\mathbf{p}(t) \equiv p_1(t) - i p_2(t)$  where  $p_1(t)$  and  $p_2(t)$  are the  $x$ - and  $y$ -components, respectively, of polar motion with the positive  $p_1$  direction being along the Greenwich meridian and the positive  $p_2$  direction being along the meridian at  $90^\circ$  W longitude,  $\chi(t) \equiv \chi_1(t) + i \chi_2(t)$  where  $\chi_1(t)$  and  $\chi_2(t)$  are the  $x$ - and  $y$ -components, respectively, of the polar motion excitation function with the positive  $\chi_1$  direction being along the Greenwich meridian and the positive  $\chi_2$  direction being along the meridian at  $90^\circ$  E longitude, and  $\sigma_{cw}$  is the complex-valued frequency of the Chandler wobble. Equation (1) is an expression of forced simple harmonic motion in the complex plane with the location of the pole in the complex plane being specified by  $\mathbf{p}(t)$  and with the right-hand-side being the forcing function. The forcing function, also known as the excitation or chi-function, is a function of the processes causing the pole position to change which in the present study is the angular momentum of the long-period ocean tides.

Comparisons between modeled and observed polar motion can be done either in the wobble domain or in the excitation domain although it is generally preferable to use the excitation domain (e.g., CHAO, 1985). Here, the comparison will be done in the excitation domain; thus, the excitation function  $\chi(t)$  must be recovered from the observed pole position  $\mathbf{p}(t)$ . The polar motion excitation data used here is that associated with SPACE95 (GROSS, 1996; GROSS, EUBANKS, STEPPE, FREEDMAN, DICKEY and RUNGE, 1997). SPACE95 is a Kalman filter-based combination of independent Earth orientation measurements taken by the space-geodetic techniques of lunar laser ranging, satellite laser ranging, very long baseline interferometry, and the global positioning system. The Kalman filter used in generating SPACE95 contains a model of the polar motion process (MORABITO, EUBANKS and STEPPE, 1988) and, besides producing daily estimates of polar motion and universal time, also produces daily estimates of the polar motion excitation functions used in this study.

A power spectrum of the SPACE95 polar motion excitation function spanning 1979-1995 is shown in Figure 1a. Positive frequencies correspond to prograde (counterclockwise) motion of

the pole in the complex plane, negative frequencies to retrograde (clockwise) motion. Spectral peaks appear at the prograde and retrograde fortnightly frequencies [ $\pm 26.7$  cycles per year (cpy)], the prograde termensual frequency (+ 40.0 cpy), but not at the monthly frequencies ( $\pm 13.3$  cpy).

### **Removal of Atmospheric Effects**

Prior to analyzing the SPACE95 polar motion excitation series for ocean tidal effects, significant sources of nonocean tidal polar motion excitation should be removed, such as those caused by atmospheric wind and pressure fluctuations. All three components of the atmospheric angular momentum (AAM) are routinely computed from products of numerical weather prediction centers and are archived at the International Earth Rotation Service (IERS) Sub-Bureau for Atmospheric Angular Momentum (SALSTEIN, KANN, MILLER and ROSEN, 1993). The particular AAM data set chosen for use here is that recently computed by SALSTEIN (1996) from the products of the National Centers for Environmental Prediction (NCEP)/ National Center for Atmospheric Research (NCAR) reanalysis system (KALNAY, KANAMITSU, KISTLER, COLLINS, DEAVEN, GANDIN, IREDELL, SAHA, WHITE, WOOLLEN, ZHU, CHELLIAH, EBISUZAKI, HIGGINS, JANOWIAK, MO, LEETMA, REYNOLDS, JENNE and JOSEPH, 1996). The NCEP / NCAR reanalysis AAM values used here span January 1, 1979 to December 31, 1995 at 6-hour intervals, have no missing values, and have no discontinuities that are commonly present in other AAM series since the atmospheric general circulation model used in the reanalysis effort was purposely frozen in order to generate homogeneous products.

SALSTEIN (1996) has computed the angular momentum associated with atmospheric pressure changes under two different assumptions for the response of the oceans to the imposed atmospheric pressure changes. The oceans are assumed to respond either as (1) an inverted barometer in which case only the mean pressure over the world's oceans is transmitted to the underlying ocean-bottom crust, or (2) a rigid body thereby fully transmitting the imposed atmospheric pressure variations to the ocean-bottom crust. At the periods of interest to this study (a week to a month) the oceans are generally believed to respond as an inverted barometer (e.g.,

DICKMAN, 1988; PONTE, SALSTEIN and ROSEN, 1991; PONTE, 1992, **1993**, 1994) and hence this version of the AAM pressure term was chosen for use here.

The total effect of atmospheric wind and pressure changes was formed by summing the AAM wind ( $w$ ) and pressure terms, with the pressure term being that computed under the inverted barometer ( $ib$ ) approximation. Daily averages of the four-times-per-day AAM values were formed with the daily averaged AAM values then linearly projected to midnight prior to their removal from the observed polar motion excitation series (which is given as daily values at midnight). Figure 1b shows the power spectrum of the residual series formed upon subtracting the resulting AAM series from the SPACE95 polar motion excitation series. Spectral peaks still appear at the prograde and retrograde fortnightly frequencies, but are no longer evident at the prograde termensual frequency (compare with Figure 1a).

### **Recovery of Ocean Tidal Terms**

Besides fitting for periodic terms at the tidal frequencies listed in Table 1, the least-squares fit to the SPACE95--AAM residual polar motion excitation series also included terms for the mean and trend of the series. The entries labeled "SP95-[w+ib]" in Table 2 give the results and  $1\sigma$  formal errors of the fit for the tidal terms at the termensual, fortnightly, and monthly frequencies in terms of the amplitude  $A$  and phase  $a$  of the prograde and retrograde components of the polar motion excitation function defined by:

$$\chi(t) = A_p e^{i\alpha_p} e^{i\phi(t)} + A_r e^{i\alpha_r} e^{-i\phi(t)} \quad (2)$$

where the subscript  $p$  denotes prograde, the subscript  $r$  denotes retrograde, and  $\phi(t)$  represents the tidal argument, the expansion of which is given in Table 1 for each tidal frequency considered here. The results of the fit at the semiannual and annual tidal frequencies are not given in Table 2 since they include such unmodeled, nonocean tidal polar motion excitation effects as seasonal changes in the wind-driven circulation of the oceans.

The two fortnightly terms, as are the two termensual terms, are close to each other in frequency, being separated by just the lunar nodal frequency  $\Omega$  (1/1 8.6 cpy; see Table 1). However, these terms have been reasonably well-resolved in the fit to the 16-year-long SPACE95–AAM residual polar motion excitation series as evidenced by an examination of the covariance matrix of the fit which shows that the largest correlation between the solved-for periodic parameters is –0.09.

Figure 1c shows the power spectrum of the post-fit residual series. As expected, there are no longer any spectral peaks at the fortnightly frequencies. Spectra (not shown) of subsets of the post-fit residual series spanning shorter lengths of time also do not exhibit peaks at the fortnightly frequencies, indicating that these signals in the SPACE95–AAM residual series (Figure 1b) are both (1) phase coherent over 1979–1 995 and (2) can be represented by the empirical model given in Table 2. The phase coherence of the fortnightly signals over a period of 16 years strongly indicates that they are of tidal origin.

Also shown in Table 2 are two additional empirical models for the effect of long-period ocean tides on polar motion excitation. The first, labeled “SP94-[w+ib]”, is that determined by GROSS, HAMDAN and BOGGS (1996) from the SPACE94–AAM residual polar motion excitation series spanning 1976.8–1 994. The AAM series used by them consisted of the sum of the wind and inverted barometer pressure terms computed from the products of the operational NCEP analysis system (not the reanalysis system whose products are used here). The second, labeled “SP95-[w+ $\gamma$ ib+(1– $\gamma$ )nib]”, is the result of testing a different method of removing atmospheric effects from the polar motion excitation series. In general, the oceans respond dynamically to imposed atmospheric pressure variations; the inverted barometer and rigid ocean assumptions are merely two extreme end-members of the spectrum of possible models for this dynamic response of the oceans. The actual response of the oceans probably lies somewhere between these two extremes. A test was therefore conducted to model the AAM pressure term as a linear combination of the pressure terms computed under the inverted barometer and rigid ocean (or no inverted barometer, nib) hypotheses. The linear combination coefficient  $\gamma$  was first determined by a

separate least-squares fit to the x- and y-components of the SPACE95 polar motion excitation series modeled as:

$$\chi_{pm} = \chi_w + \gamma \chi_{ib} + (1 - \gamma) \chi_{nib} \quad (3)$$

where  $\chi_{pm}$  is either the x- or y-component of the SPACE95 polar motion excitation series,  $\chi_w$  is that respective component of the AAM wind term computed from the NCEP / NCAR reanalysis products,  $\chi_{ib}$  is that respective component of the AAM pressure term computed under the inverted barometer assumption, and  $\chi_{nib}$  is that respective component of the AAM pressure term computed under the rigid ocean, or no inverted barometer, assumption. The value obtained for the linear combination coefficient  $\gamma$  was 0.7603 for the x-component and 0.4947 for the y-component. The empirical model for the effect of long-period ocean tides on polar motion excitation obtained by removing this linear combination of the atmospheric wind and pressure terms from the SPACE95 polar motion excitation series prior to solving for the tidal terms is reported in Table 2 under the entries labeled "SP95-[w+ $\gamma$ ib+(1- $\gamma$ )nib]".

As can be seen from Table 2, the various estimates for the observed effect of long-period ocean tides on polar motion excitation agree with each other to within about  $1 - 2\sigma$ , with the various estimates at the fortnightly frequencies agreeing with each other to within about 10. The preferred empirical model, however, is that resulting from removing the sum of the AAM wind and inverted barometer pressure terms from the SPACE95 polar motion excitation series since these results generally have the smallest formal uncertainties. Furthermore, since the formal uncertainties are computed from the root-mean-square (rms) scatter of the post-fit residual series, the results with the smallest formal uncertainties will be those determined from the series with the smallest rms scatter, that is, from the series that has had atmospheric effects removed most completely. Thus, at the frequencies of interest here, atmospheric effects are better modeled by taking the sum of the wind and inverted barometer pressure terms than they are by taking the sum of the wind and the best-fitting linear combination of inverted barometer and no inverted barometer pressure terms. This is confirmed by an examination (not shown) of power spectra of the respective SPACE95-

AAM residual series which indicates generally smaller power in that series from which the sum of the wind and inverted barometer pressure terms has been removed.

## MODEL PREDICTIONS

The predictions of three different ocean tide models for the effect of long-period ocean tides on polar motion excitation are also given in Table 2. The first two predictions are from purely hydrodynamic ocean tide models: that of DICKMAN (1993), and that of Brosche as analyzed by SEILER (1991) for ocean tidal angular momenta and subsequently by GROSS (1993) and BROSCHE and WÜNSCH (1994) for the ocean tidal effect on polar motion (the entries in Table 2 for the predictions of these two ocean tide models have been reproduced here from those given by GROSS, HAMDAN and BOGGS (1996) where greater discussion of these model predictions can be found). The third ocean tide model whose polar motion excitation predictions are listed in Table 2 is that of DESAI (1996) whose model has had Topex sea surface height measurements assimilated into it. Two different results from Desai's model are listed in Table 2 corresponding to two different time spans of Topex data assimilation: Topex repeat cycles 10-110 (approximately 1000 days), and Topex repeat cycles 10-130 (approximately 1200 days). Since the alias frequency of the termensual  $Mt$  tide in the Topex measurements is 115.7 days (DESAI, 1996, Table 6.2), no predictions for the effect on polar motion excitation of the termensual tides are given since the Topex measurements spanning repeat cycles 10-130 are long enough to sense only about 10 oscillations of the aliased  $M?$  tide. Since the monthly  $Mm$  tide is not aliased in Topex measurements because its period of 27.6 days is greater than twice the exact repeat period of Topex (9.9156 days), and since the alias frequency of the fortnightly  $Mf$  tide is 36.2 days, about 40 oscillations of the  $Mm$  and aliased  $Mf$  tides are contained in the Topex measurements spanning repeat cycles 10-130. However, as discussed below, even 40 tidal oscillations are not enough to generate predictions that have converged (see Figure 2).

The convergence properties of the predictions of Desai's model are illustrated in the phasor diagrams of Figure 2 which show the amplitude and phase of the predicted effect of the  $Mm$  and

*Mf* ocean tides on polar motion as a function of the amount of Topex data that has been assimilated. The effect on polar motion  $\mathbf{p}(t)$  was recovered from the effect on polar motion excitation  $\chi(t)$  by solving equation (1) with the excitation function given by equation (2). The numerical labels in Figure 2 indicate the amount of Topex data that has been assimilated. For example, the arrows labeled “50” have had measurements from Topex cycles 10–50 assimilated into the ocean tide model, those labeled “60” have had measurements from cycles 10–60 assimilated, etc. Also indicated in Figure 2 are the predictions, labeled “B”, of the Brosche tide model, and the observed results, labeled “O”, of GROSS, HAMDAN and BOGGS (1996). As can be seen, the effects of the *Mf* and *Mm* ocean tides on polar motion as predicted by the Desai model are still changing as additional Topex measurements are assimilated into the model, indicating that the predictions of the Desai model have not yet converged. In the most extreme case illustrated, the phase of the predicted *Mm* retrograde tidal effect changes by nearly  $180^\circ$  as sea surface height measurements from 10 additional Topex cycles (120–130) are assimilated into the model.

## DISCUSSION

In Figure 1 b spectral peaks are clearly evident at the fortnightly tidal frequencies having corresponding amplitude signal-to-noise ratios of about 5 at the prograde *Mf* tidal frequency, and about 8 at the retrograde *Mf* tidal frequency (see Table 2 entries labeled "SP95-[w+ib]"). The different empirical models for the effect of ocean tides on polar motion excitation, based upon different observed polar motion excitation series and different methods of removing atmospheric effects, agree with each other at the fortnightly frequencies to within about 10. However, as can be seen from Table 2, the predictions at the fortnightly frequencies of the different ocean tide models differ from each other and from the observations by up to a factor of 2 in amplitude, and more than  $100^\circ$  in phase. This illustrates the need for better models of the effect of long-period ocean tides on polar motion excitation. Fortunately, the Desai ocean tide model can be expected to yield improved results since its predictions to date have not yet converged. Convergence can be achieved by assimilating more Topex measurements into the model. Also, the path to convergence

can be shortened by accounting for the effects of wind-driven sea surface height changes on the Topex measurements prior to their assimilation into the ocean tide model. This can be accomplished by using the sea surface height products of realistic wind-driven general ocean circulation models such as that of SEMTNER and CHERVIN (1992).

In addition, better observations of the effect of the fortnightly ocean tides on polar motion excitation are needed. In principle, the oceans should have the same response to the tidal potential at the  $Mf$  and  $Mf'$  tidal frequencies since these frequencies are so close to each other, differing by only  $1/18.6$  cpy. This implies that the phase of the effect of the  $Mf$  ocean tide on polar motion excitation should be the same as that of the effect of the  $Mf'$  ocean tide, and that the ratio of their amplitudes should be the same as the ratio of the amplitudes of the tidal potential at these frequencies. However, from the entries in Table 2 for the preferred empirical model (labeled "SP95-[w+ib]") it is seen that this is not the case. The  $Mf-Mf'$  difference of the prograde and retrograde phases are seen to be  $86^\circ$  and  $-38^\circ$ , respectively, and the prograde and retrograde  $Mf/Mf'$  amplitude ratios, which should each be 2.4 (e.g., CARTWRIGHT and ED DEN 1973, Table 1a), are 1.2 and 1.9, respectively. Improved observations of the effect of the fortnightly ocean tides on polar motion excitation will be obtained as additional high-quality, space-geodetic measurements are made. Also, during the least-squares fit to the residual polar motion excitation series, constraints could be placed on the solution forcing the recovered  $Mf$  and  $Mf'$  tidal terms to have the same phase and the expected amplitude ratio of 2.4.

**Acknowledgments.** The work described in this paper was partially performed at the Jet Propulsion Laboratory, California Institute of Technology, under contract with the National Aeronautics and Space Administration.

## REFERENCES

- BROSCHÉ, P. and J. WÜNSCH (1994) On the “rotational angular momentum” of the oceans and the corresponding polar motion. *Astronomische Nachrichten*, **315**, 181–188.
- CARTWRIGHT, D. E. and A. C. EDDEN (1973) Corrected tables of tidal harmonics. *Geophysical Journal of the Royal Astronomical Society*, **33**, 253-264.
- CHAO, B. F. (1985) On the excitation of the Earth’s polar motion. *Geophysical Research Letters*, **12**, 526-529.
- CHAO, B. F. (1994) Zonal tidal signals in the Earth’s polar motion (abstract). *Eos Transactions of the American Geophysical Union*, 75(44), Fall Meeting Suppl., 158.
- DESAI, S. D. (1996) Ocean tides from Topex/Poseidon altimetry with some geophysical applications. Ph.D. thesis, Univ. of Colo., 254 pp.
- DICKMAN, S. R. (1988) Theoretical investigation of the oceanic inverted barometer response. *Journal of Geophysical Research*, 93, 14941–14946.
- DICKMAN, S. R. (1993) Dynamic ocean-tide effects on Earth’s rotation. *Geophysical Journal International*, 112, 448-470.
- EUBANKS, T. M. (1993) Variations in the orientation of the Earth. In: *Contributions of Space Geodesy to Geodynamics: Earth Dynamics*, D. E. SMITH and D. L. TURCOTTE, editors, American Geophysical Union Geodynamics Series, 24, pp. 1–54.
- GROSS, R. S. (1992) Correspondence between theory and observations of polar motion. *Geophysical Journal International*, **109**, 162-170.
- GROSS, R. S. (1993) The effect of ocean tides on the Earth’s rotation as predicted by the results of an ocean tide model. *Geophysical Research Letters*, 20, 293–296.
- GROSS, R. S. (1996) A combination of EOP measurements: SPACE95. In: *Earth Orientation and Reference Frames Submitted for the 1995 IERS Annual Report*, IERS Tech. Note 22, P. CHARLOT, editor, Obs. de Paris, in press.

- GROSS, R. S., K. H. HAMDAN and D. H. BOGGS (1996) Evidence for excitation of polar motion by fortnightly ocean tides. *Journal of Geophysical Research*, **23**, 1809--1812.
- GROSS, R. S., T. M. EUBANKS, J. A. STEPPE, A. P. FREEDMAN, J. O. DICKEY and T. F. RUNGE (1997) A Kalman filter-based approach to combining independent Earth orientation series. *Journal of Geodesy*, submitted.
- HERRING, T. A. (1993) Diurnal and semidiurnal variations in Earth rotation. In: *Observations of Earth from Space*, R. P. SINGH, M. FEISSEL, B. D. TAPLEY and C. K. SHUM, editors, Advances in Space Research, **13**, Pergamon, pp. (11 )28 1--(11 )290.
- HERRING, T. A. and D. DONG (1994) Measurement of diurnal and semidiurnal rotational variations and tidal parameters of Earth. *Journal of Geophysical Research*, **99**, 18051 – 18071.
- KALNAY, E., M. KANAMITSU, R. KISTLER, W. COLLINS, D. DEAVEN, L. GANDIN, M. IREDELL, S. SAHA, G. WHITE, J. WOOLLEN, Y. ZHU, M. CHELLIAH, W. EBISUZAKI, W. HIGGINS, J. JANOWIAK, K. C. MO, A. LEETMA, R. REYNOLDS, R. JENNE and D. JOSEPH (1996) The NCEP/NCAR 40-year Reanalysis Project. *Bulletin of the American Meteorological Society*, **77**, 437-471.
- LAMBECK, K. (1980) *The Earth's Variable Rotation: Geophysical Causes and Consequences*, Cambridge University Press, 449 pp.
- LAMBECK, K. (1988) *Geophysical Geodesy: The Slow Deformations of the Earth*, Oxford University Press, 718 pp.
- MORABITO, D. D., T. M. EUBANKS and J. A. STEPPE (1988) Kalman filtering, of Earth orientation changes. In: *The Earth's Rotation and Reference Frames for Geodesy and Geodynamics*, A. K. BABCOCK and G. A. WILKINS, editors, D. Reidel, pp. 257–267.
- MORITZ, H. and I. I. MUELLER (1988) *Earth Rotation: Theory and Observation*, Ungar, 617 pp.
- MUNK, W. H. and G. J. F. MACDONALD (1960) *The Rotation of the Earth: A Geophysical Discussion*, Cambridge University Press, 323 pp.

- PONTE, R. M. (1992) The sea level response of a stratified ocean to barometric pressure forcing. *Journal of Physical Oceanography*, 22, 109-113.
- PONTE, R. M. (1993) Variability in a homogeneous global ocean forced by barometric pressure. *Dynamics of Atmospheres and Oceans*, 18, 209-234.
- PONTE, R. M. (1994) Understanding the relation between wind- and pressure-driven sea level variability. *Journal of Geophysical Research*, 99, 8033-8039.
- PONTE, R. M., D. A. SALSTEIN and R. D. ROSEN (1991) Sea level response to pressure forcing in a barotropic numerical model. *Journal of Physical Oceanography*, 21, 1043- 1057.
- SALSTEIN, D. A. (1996) Sub-bureau for Atmospheric Angular Momentum. In: 1995 IERS Annual Report, Ohs. de Paris, pp. 1117-11115.
- SALSTEIN, D. A., D. M. KANN, A. J. MILLER and R. D. ROSEN (1993) The Sub-bureau for Atmospheric Angular Momentum of the International Earth Rotation Service: A Meteorological Data Center with Geodetic Applications. *Bulletin of the American Meteorological Society*, 74, 67-80.
- SEILER, U. (1991) Periodic changes of the angular momentum budget due to the tides of the world ocean. *Journal of Geophysical Research*, 96, 10287-10300.
- SEMTNER, A. J. and R. M. CHERVIN (1992) Ocean general circulation from a global eddy-resolving model. *Journal of Geophysical Research*, 97, 5493-5550.
- SOVERS, O. J., C. S. JACOBS and R. S. GROSS Measuring rapid ocean tidal Earth orientation variations with VLBI. *Journal of Geophysical Research*, 98, 19959- 19971, 1993.
- WATKINS, M. M. and R. J. EANES (1994) Diurnal and semidiurnal variations in Earth orientation determined from LAGEOS laser ranging. *Journal of Geophysics/ Research*, 99, 18073-18079.
- YODER, C. F., J. G. WILLIAMS and M. E. PARKE (1981) Tidal variations of Earth rotation. *Journal of Geophysical Research*, 86, 881--891.

## FIGURE CAPTIONS

**Figure 1.** Power spectral density (psd) estimates (periodograms) in decibels (db) computed from time series of polar motion excitation functions  $\chi(t)$  spanning 1979–1995 of (a) the SPACE95 polar motion excitation function derived from space-geodetic Earth rotation measurements, (b) the residual polar motion excitation function formed by subtracting atmospheric effects from the SPACE95 excitation series, and (c) the result of removing the recovered tidal terms from the SPACE95–AAM residual series. The vertical dotted lines indicate frequencies in the prograde and retrograde termensual tidal bands (at  $\pm 40.0$  cpy), fortnightly tidal bands (at  $\pm 26.7$  cpy), and monthly tidal bands (at  $\pm 13.3$  cpy). The retrograde (clockwise) component of polar motion excitation is represented by negative frequencies, the prograde (counterclockwise) component by positive frequencies.

**Figure 2.** Phasor diagrams of the amplitude and phase of the effect on polar motion of the  $Mf$  and  $Mm$  ocean tides predicted by the DESAI (1996) ocean tide model as a function of the amount of Topex data that has been assimilated into the model. Arrows labeled “50” have had sea surface height measurements from Topex repeat cycles 10–50 assimilated into the model, “60” have had cycles 10–60 assimilated, etc. The arrows labeled “B” are the predictions of the Brosche model as tabulated by GROSS (1993). The arrows labeled “O” are the observed results of GROSS, HAMDAN and BOGGS (1996). Note that the results illustrated here are for the effect of the  $Mf$  and  $Mm$  ocean tides on polar motion  $\mathbf{p}(t)$ , whereas the results tabulated in Table 2 are for the effect on polar motion excitation  $\chi(t)$ .

**Table 1.** Expansion of the Tidal Argument

Tide	Period (solar days)	Fundamental Argument				
		1	1'	$F$	$D$	$\Omega$
Termensual						
<i>Mt'</i>	9.12	1	0	2	0	1
<i>Mt</i>	9.13	1	0	2	0	2
Fortnightly						
<i>Mf'</i>	13.63	0	0	2	0	1
<i>Mf</i>	13.66	0	0	2	0	2
Monthly						
<i>Mm</i>	27.55	1	0	0	0	0
Semiannual						
<i>Ssa</i>	182.62	0	0	2-2		2
Annual						
<i>Sa</i>	365.26	0	1	0	0	0

**Table 2.** Observed and Predicted Effects of Long-Period Ocean Tides on the Polar Motion Excitation Function  $\chi(t)$

	Prograde		Retrograde	
	Amplitude (mas)	Phase (degrees)	Amplitude (mas)	Phase (degrees)
<i>Mt'</i> (9.12-day)				
SP95-[w+ib]	<b>0.682:0.30</b>	$-6 \pm 25$	$0.60 \pm 0.30$	$141 \pm 28$
SP95-[w+ $\gamma$ ib+(1- $\gamma$ ) nib]	<b>0.55 <math>\pm</math> 0.31</b>	$1 \pm 32$	$0.50 \pm 0.31$	$123 \pm 36$
SP94-[w+ib] <sup>1</sup>	$0.54 \pm 0.45$	$38 \pm 48$	$0.215:0.45$	$79 \pm 126$
Dickman model <sup>2</sup>	0.13	73	0.21	15
<i>Mt</i> (9.13-day)				
SP95-[w+ib]	$0.22 \pm 0.30$	$19 \pm 78$	$0.33 \pm 0.30$	$-37 \pm 52$
SP95-[w+ $\gamma$ ib+(1- $\gamma$ ) nib]	$0.16 \pm 0.31$	$19 \pm 115$	$0.41 \pm 0.31$	$-78 \pm 44$
SP94-[w+ib] <sup>1</sup>	$0.47 \pm 0.45$	$-30 \pm 55$	$0.41 \pm 0.45$	$-95 \pm 63$
Dickman model <sup>2</sup>	0.32	73	0.52	15
<i>Mf'</i> (13.63-day)				
SP95-[w+ib]	$1.37 \pm 0.30$	$30 \pm 13$	$1.36 \pm 0.30$	$69 \pm 13$
SP95-[w+ $\gamma$ ib+(1- $\gamma$ ) nib]	$1.27 \pm 0.31$	$30 \pm 14$	$1.50 \pm 0.31$	$59 \pm 12$
SP94-[w+ib] <sup>1</sup>	$1.61 \pm 0.45$	$56 \pm 16$	$2.01 \pm 0.45$	$87 \pm 13$
Dickman model <sup>2</sup>	0.52	100	0.71	8
Brosche/Seiler/Gross model <sup>3</sup>	0.72	55	0.59	72
<i>Mf</i> (13.66-day)				
SP95-[w+ib]	$1.69 \pm 0.30$	$116 \pm 10$	$2.58 \pm 0.30$	$31 \pm 7$
SP95-[w+ $\gamma$ ib+(1- $\gamma$ ) nib]	$1.60 \pm 0.31$	$116 \pm 11$	$2.59 \pm 0.31$	$36 \pm 7$
SP94-[w+ib] <sup>1</sup>	$0.86 \pm 0.45$	$93 \pm 30$	$2.73 \pm 0.45$	$14 \pm 10$
Dickman model <sup>2</sup>	1.26	100	1.72	8
Brosche/Seiler/Gross model <sup>3</sup>	1.72	55	1.44	72
Desai model (Topex 10-1 10) <sup>4</sup>	3.41	158	1.73	-4
Desai model (Topex 10-1 30)	3.07	170	2.45	4
<i>Mm</i> (27.55-day)				
SP95-[w+ib]	$0.65 \pm 0.30$	$95 \pm 26$	$0.98 \pm 0.30$	$-55 \pm 17$
SP95-[w+ $\gamma$ ib+(1- $\gamma$ ) nib]	$0.61 \pm 0.31$	$140 \pm 30$	$0.88 \pm 0.31$	$-53 \pm 20$
SP94-[w+ib] <sup>1</sup>	$0.75 \pm 0.45$	$49 \pm 35$	$0.82 \pm 0.45$	$-59 \pm 32$
Dickman model <sup>2</sup>	0.47	136	0.28	-7
Brosche/Seiler/Gross model <sup>3</sup>	0.78	74	0.92	28
Desai model (Topex 10-1 10) <sup>4</sup>	1.15	-50	0.90	153
Desai model (Topex 10-1 30)	1.22	-34	0.43	24

<sup>1</sup>As reported by GROSS, HAMDAN and BOGGS (1996).

<sup>2</sup>From the ocean tidal effect on polar motion reported by DICKMAN (1993). See GROSS, HAMDAN and BOGGS (1996) for a discussion of these results.

<sup>3</sup>From the ocean tidal effect on polar motion reported by GROSS (1993) and computed from the angular momenta of the Brosche ocean tide model as tabulated by SEILER (1993).

<sup>4</sup>From the ocean tidal effect on polar motion reported by DESAI (1996).

# POLAR MOTION EXCITATION SPECTRA (1979-1995)

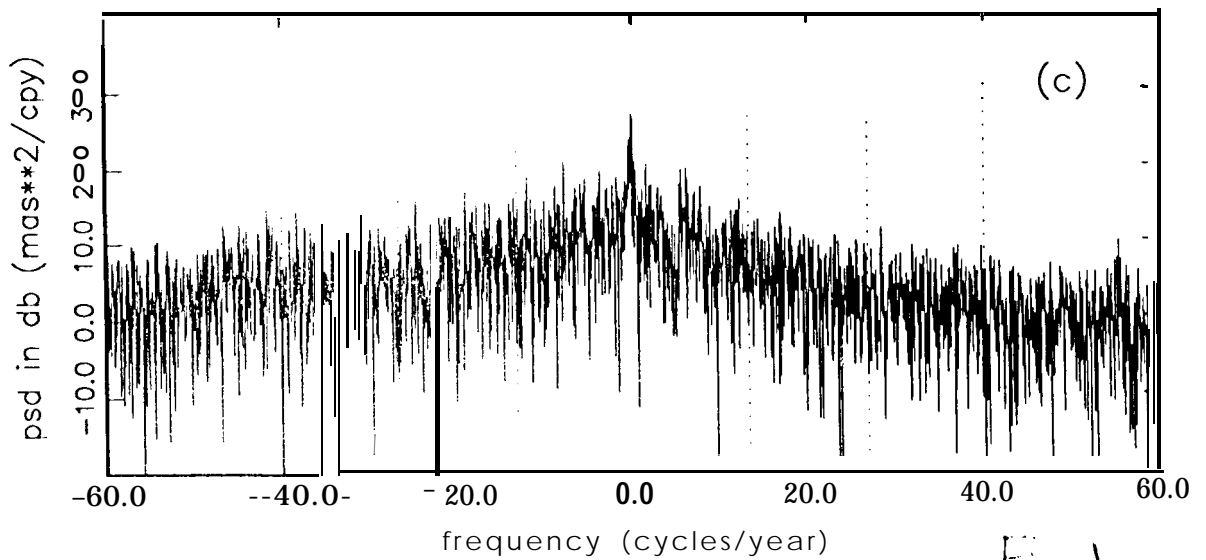
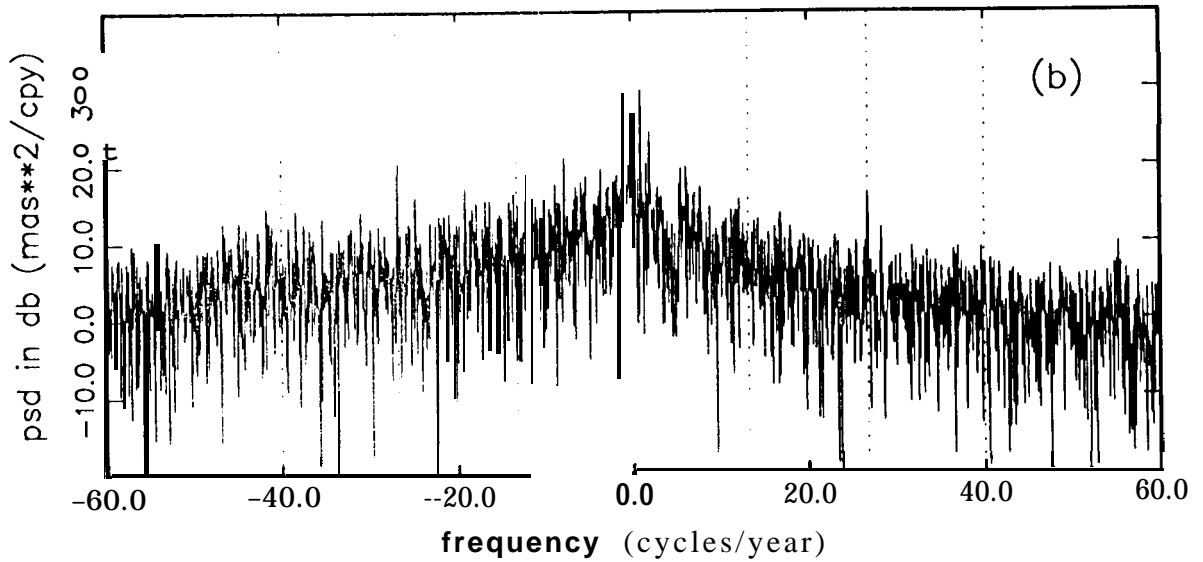
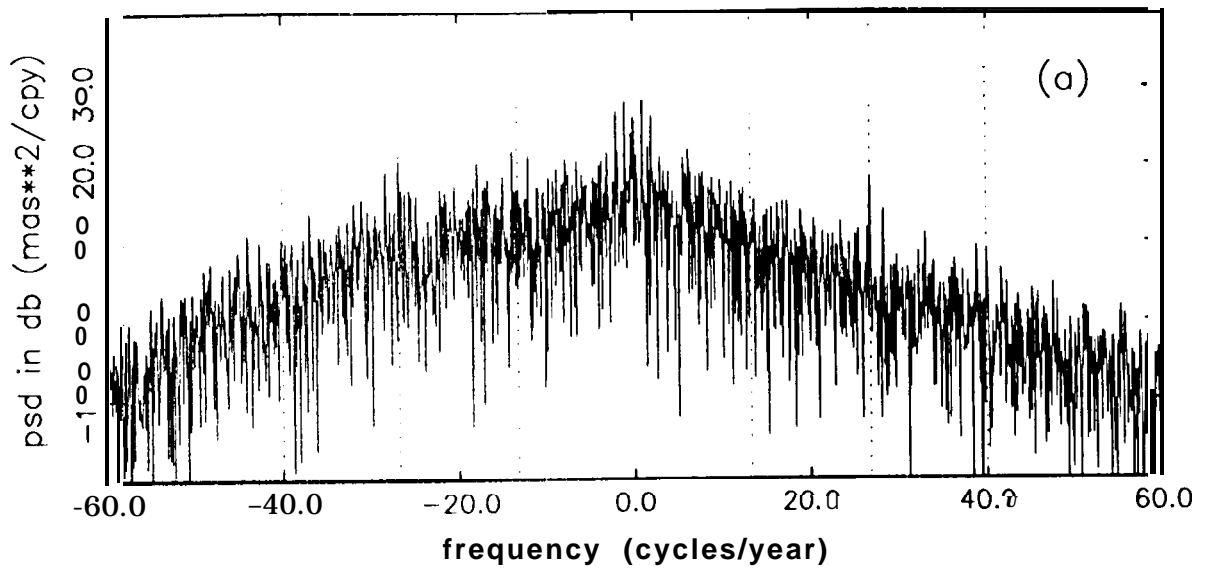


Fig. 1

# Polar Motion Observations and Ocean Tide Predictions

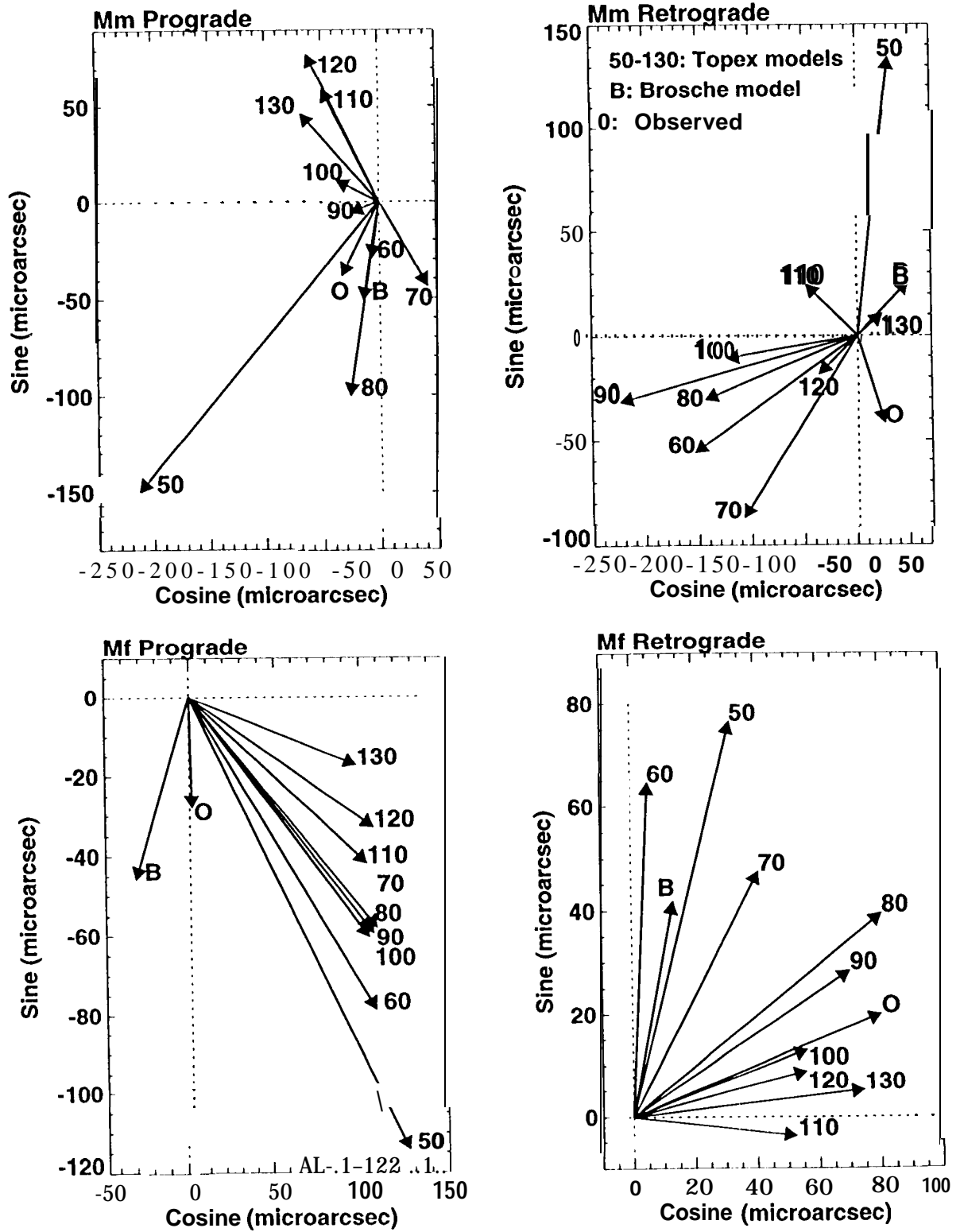


Fig. 2